RSC Advances

PAPER

View Article Online
View Journal | View Issue

Cite this: *RSC Adv.*, 2024, **14**, 8726

Developing a novel magnetic organic polymer for selective extraction and determination of 16 macrolides in water and honey samples†

Mengnan Liang,[a] Na Li,[a] Hao Zhang,[a] Ling Ma*[bc] and Ke Wang *[abc]

Received 19th January 2024
Accepted 3rd March 2024

DOI: 10.1039/d4ra00496e

rsc.li/rsc-advances

A novel magnetic organic polymer Fe_3O_4@SiO_2@Tb–PDAN was designed and synthesized, which was used as an adsorbent for magnetic solid-phase extraction (MSPE) of 16 macrolides (MALs) in water and honey. The synthesized adsorbent was characterized using techniques including scanning electron microscopy (SEM), Fourier transform infrared spectroscopy (FT-IR) and X-ray diffraction (XRD). Then several parameters of the extraction process were further optimized. Under the optimized conditions, an MSPE-LC-MS/MS method was established for extraction and determination of 16 MALs, which showed good linearity ($r \geq 0.999$), low limits of detection (0.001–0.012 μg L^{-1} for water and 0.001–0.367 μg kg^{-1} for honey) and satisfactory recoveries (70.02–118.91%) with the relative standard deviations (RSDs) lower than 10.0%. This established method was then successfully applied to detect MALs in real samples, which suggested that Fe_3O_4@SiO_2@Tb–PDAN was a potential magnetic adsorbent for efficient extraction and analysis of MALs.

1. Introduction

Macrolides (MALs) are lipophilic and basic antibiotics produced by *Streptomyces* species, which consist of a 12–16-membered large central ring and one or more sugars connected to the lactone ring *via* a glycosylic bond.[1] They have been used since their discovery over half a century ago. Currently, MALs are widely used in clinical treatment[2–6] and are gradually expanding to other fields.[7–10] Nonetheless, incorrect use of MALs can lead to their residues in the environment and food samples, including water,[11–13] honey,[14,15] dairy products[16–18] and meat.[19,20] Once these residues are ingested by the human body through the food chain and accumulate to a certain concentration, MALs and their metabolites may cause hearing loss and impaired vestibular function.[21] Besides, they also interfere with normal heart,[22] liver and kidney function,[23] and even lead to an increasing number of resistant bacteria in the body. Given the seriousness of the situation, several countries and organizations, including the USA, the European Union and China, have set maximum residue limits (MRLs) for MALs in animal tissue for human consumption.[24] Hence, it is of great necessity to develop quick and effective methods for detecting MALs.

Various techniques have been proposed for the analysis of MALs such as capillary electrophoresis (CE),[25] immunogold chromatographic assay (IGCA),[26] thin-layer chromatography (TLC)[27] and liquid chromatography-tandem mass spectrometry (LC-MS/MS).[28,29] Among these methods, LC-MS/MS is the most popular technique due to its sensitivity, specificity and ability.[30] Up to now, the technique has been applied for the determination of different samples. However, due to the complex matrix of real samples, it is still difficult to determine low concentrations of analytes in samples. Therefore, sample pretreatment is often an essential procedure prior to instrumental analysis. To date, there are many sample pretreatment methods for MALs, such as liquid–liquid extraction (LLE),[31] dispersive liquid–liquid microextraction (DLLME),[32] solid-phase extraction (SPE),[33] dispersive solid-phase extraction (DSPE)[34] and magnetic solid-phase extraction (MSPE).[35] Compared to other methods, MSPE is an attractive technique due to its low consumption of organic solvents. Additionally, it can isolate target components by using an external magnetic field for the separation of target components, eliminating the need for laborious and time-consuming conventional centrifugation methods.[36] In MSPE, a magnetic sorbent plays a significant role in extraction efficiency and selectivity.

Nowadays, a variety of adsorbents have been designed and synthesized for extraction of variety of pollutants, including metal organic frameworks,[37] covalent organic frameworks,[38] molecularly imprinted polymers[39] and other polymers.[40] However, their isolation and recovery from samples is a challenge that somewhat limits their application in wider fields.

[a]*College of Chemistry and Materials Science, Hebei Normal University, Shijiazhuang 050023, China. E-mail: wkecdc@163.com*

[b]*Shijiazhuang Center for Disease Control and Prevention, Shijiazhuang 050011, China. E-mail: mamalin001@163.com*

[c]*Shijiazhuang Technology Innovation Center for Chemical Poison Detection and Risk Early Warning, Shijiazhuang 050011, China*

† Electronic supplementary information (ESI) available. See DOI: https://doi.org/10.1039/d4ra00496e

Therefore, Fe_3O_4 magnetic nanoparticles have been introduced in adsorbents to synthesize magnetic materials with stability, selectivity and simple separation, which is the way to solve the above problems.[41] Wang *et al.* prepared magnetic particles (IRMOF-3 coated SiO_2/Fe_3O_4) as adsorbents for MSPE and combined with LC-MS/MS for the analysis of ten quinolones in water and a fish sample.[42] Yu *et al.* synthesized a magnetic covalent organic framework using 2,4,6-trihydroxybenzene-1,3,5-tricarbaldehyde (Tp) and *p*-phenylenediamine (Pa-1), which displayed great magnetic responsiveness and good thermal stability and was used for the extraction of aromatic amine metabolites in urine.[43] Magnetic molecularly imprinted polymers were fabricated and used as efficient adsorbents to extract MALs from food samples by Zhou *et al.*[24] Li *et al.* synthesized a magnetic knitting aromatic polymer to develop a method for the simultaneous determination of six benzoylurea insecticides in honey and juice samples.[44]

Even though magnetic adsorbents have been developed for the extraction of pollutants, they are still at an infant stage. Currently, the synthesis of magnetic adsorbents based on good selectivity is generating a great research interest and attracting more and more attention. Designing the adsorbent according to the properties of the analyte improves the separation selectivity and facilitates the extraction of analytes from complex samples.[45] MALs are hydrophobic and their chemical structure contains unsaturated bonds. In light of these considerations, the study designed and synthesized a novel magnetic organic polymer Fe_3O_4@SiO_2@Tb–PDAN, which was prepared from magnetic Fe_3O_4, 1,3,5-triformylbenzene (Tb) and 1,4-phenylenediacetonitrile (PDAN). It contains cyano groups and benzene rings, connected by C=C bonds, exhibiting a conjugated planar structure, which facilitates adsorption with MALs molecules through intermolecular forces and hydrophobic interactions.

Herin, a high-throughput method based on MSPE with Fe_3O_4@SiO_2@Tb–PDAN followed by LC-MS/MS determination was established which was validated and applied to determine 16 MALs in water and honey samples. Major conditions that may affect the efficiency of MSPE were optimized, including adsorbent dosage, sample solution pH, salt concentration, extraction time, eluent, volume of eluent and desorption time. The proposed method was sensitivity, selectivity and accuracy in the simultaneous determination of these MALs.

2. Experimental

2.1. Reagents and materials

Ferric chloride hexahydrate ($FeCl_3 \cdot 6H_2O$), ethylene glycol (EG), sodium acetate trihydrate ($NaAc \cdot 3H_2O$) and anhydrous ethanol were purchased from Tianjin Yong da Chemical Reagent Co., Ltd (Tianjin, China). Tb, PDAN, tetrahydrofuran (THF) and 1,8-diazabicyclo-[5,4,0]undec-7-ene (DBU) were offered by Aladdin Chemistry Co., Ltd (Shanghai, China). Tetraethoxysilane (TEOS) was obtained from Analysis of Pure Sinopharm Group Chemical Reagent Co. Ltd (Shanghai, China). Polyethylene glycol (PEG-4000) was supplied by Xiya Chemical Technology Co. Ltd (Shandong, China). Aqueous ammonia (25 wt%) and sodium chloride (NaCl) were acquired from Tianjin Kermel Chemical Reagent Co., Ltd (Tianjin, China). 99.9% (w/w) formic acid was purchased from Dikma (Lake Forest, USA). Acetonitrile (ACN) was obtained from obtained from Merck (Darmstadt, Germany). Methanol (MA), acetone (AC) and ethyl acetate were purchased from Thermo Fisher Co., Ltd (Waltham, USA). MA and ACN were of HPLC grade, and other reagents were of analytical grade. Ultra-pure water was prepared using a Millipore Milli-Q Gradient Water Purification System (USA).

Clindamycin, tilmicosin, erythromycin, clarithromycin, roxithromycin, eprinomectin, avermectin, doramectin, emamectin, ivermectin, selamectin, and moximycin were purchased from Dr Ehrenstorfer GmbH (Augsburg, Germany). Oleandomycin was obtained from MedChemExpress. Anhydroerythromycin A, Erythromycin A enol ether and Oleandomycin triacetate were acquired from Toronto Research Chemicals. Details of 16 MALs are shown in the Table S1.† The standard stock solutions (1000 mg L^{-1}) containing 16 MALs were prepared in ACN at −20 °C. The working standard solutions were diluted gradually with a 7 : 3 (v/v) mixture of ACN and 0.1% formic acid solution to prepare solvent calibration standards to obtain different concentrations. Matrix-matched calibration standard solutions were prepared by adding different amounts of working standard solutions in blank matrix solution.

2.2. Instrumental and analytical conditions

Analysis and detection were performed on an UPLC-MS/MS instrument (Exion TRILPLE QUAD 5500, AB SCIEX, USA). A Phenomenex Kinetex F5 100 Å (3.0 mm × 100 mm, 2.6 μm particle diameter) was used for separation of analytes at a constant column temperature of 40 °C. Using 0.1% formic acid water (mobile phase A)-acetonitrile (mobile phase B) as the mobile phase, the flow rate was 0.3 mL min^{-1}, and the sample size was 3.0 μL. The gradient program was as follows: 0–0.5 min 30% B; 0.5–3.0 min 32% B; 3.0–6.0 min 45% B; 6.0–9.5 min 78% B, 9.5–12 min 30% B. Chromatograms of 16 MALs was depicted in Fig. S1.† Mass spectrometer was configured to collect data in the multiple reaction monitoring (MRM) mode with electrospray ionization source (ESI) in positive ion. The spray voltage was 5500 V. The vaporizer temperature was 550 °C. Nebulizing gas pressure, auxiliary gas pressure, and curtain gas pressure were 55 psi, 55 psi and 40 psi. Table S2† presents retention times, precursor ion, product ion, declustering potential (DP) and collision energy (CE) for each target analyte.

X-ray diffraction (XRD) measurements were made using a German Bruker D8 ADVANCE diffractometer. Fourier transform infrared spectroscopy (FT-IR) is measured on the iS5 infrared spectrometer (Thermo Nicolet, USA). Regulus 8100 scanning electron microscopy (SEM) (Hitachi, Japan) and Tecnai G2 F20 transmission electron microscopy (TEM) (FEI, USA) were used to observe the morphology. The magnetic properties were analysed by an MPMS (SQUID) XL-7 vibration sample magnetometer (VSM) (Quantum Design, USA).

2.3. Synthesis of Fe_3O_4@SiO_2@Tb–PDAN

Magnetic Fe_3O_4 nanoparticles were prepared with reference to previous reports.[46] In short, 1.62 g $FeCl_3 \cdot H_2O$ was dispersed

evenly in 60 mL EG under magnetic stirring. Next, 2.0 g PEG-4000 and 7.2 g $CH_3COONa{\cdot}3H_2O$ were added successively. The mixture was stirred for 30 min under the action of a magnetic stirrer to obtain a homogeneous solution. Then the mixed solution was transferred to a Teflon-lined stainless-steel autoclave and stored at 200 °C for 8 hours. After falling to room temperature, the precipitation was collected by magnets and washed several times with ultrapure water and ethanol. Finally, the black product was dried overnight at 60 °C in a vacuum for later use.

The obtained Fe_3O_4 nanoparticles were coated with SiO_2 layer according to the previous report.[47] Typically, the 200 mg Fe_3O_4 nanoparticles were added to a mixture of 160 mL ethanol and 40 mL ultrapure water. The mixture was sonicated for 30 min to ensure full dispersion. Next, 3 mL aqueous ammonia was added to the mixture and ultrasound was performed for 5 min. Then 2.0 mL TEOS was added dropwise to the mixture and reacted for 24 hours at 30 °C to get Fe_3O_4@SiO_2. The product was collected with an external magnetic field, washed with ultrapure water and ethanol several times and dried in a vacuum at 60 °C for 4 hours.

Fe_3O_4@SiO_2@Tb–PDAN was synthesized according to a modified method.[48] First, 100 mg Fe_3O_4@SiO_2 was added to 20 mL THF and ultrasounded for 5 min. Then, 51.9 mg Tb and 75.0 mg PDAN were added to the above mixture successively and stirred, and then 2 mL DBU (6 mol L^{-1}) was added to react at reflow temperature for 24 hours. The product was washed with anhydrous ethanol for several times and dried in a vacuum at 60 °C for further use.

2.4. Sample preparation

The water samples were stored at 4 °C and filtered through the 0.45 μm nylon membrane. Surface water samples spiked with appropriate volumes of MALs stock solution were used for the method optimization and validation experiments. 1.0 g of honey sample was dissolved in ultrapure water and marked to 50.0 mL. All the samples were adjusted to pH = 8 before MSPE.

2.5. Procedure of MSPE

The procedure of MSPE (Fig. 1) was carried out as follows: firstly, 12.0 mg of Fe_3O_4@SiO_2@Tb–PDAN was added into a 50 mL centrifuge tube containing 10.0 mL of sample solution at room temperature. Next, the centrifuge tube was put on a vortex oscillator device for 5 min to achieve the adsorption of MALs from sample solution onto Fe_3O_4@SiO_2@Tb–PDAN. Afterward, a magnet was employed for collecting the magnetic material, and the supernatants were decanted directly. Subsequently, 6 mL of 0.3% ammoniated ACN was added into the collected magnetic material and vortex for 5 min to elute MALs. Then the eluate was collected under an external magnetic field and the elution was repeated once. After that, it was collected in a 15 mL tube and evaporated to dryness in a stream of nitrogen gas. Finally, the eluate was redissolved with 1 mL of mobile phases A and B mixture (v/v = 3 : 7) and filtered with 0.20 μm nylon membrane for subsequent LC-MS/MS analysis.

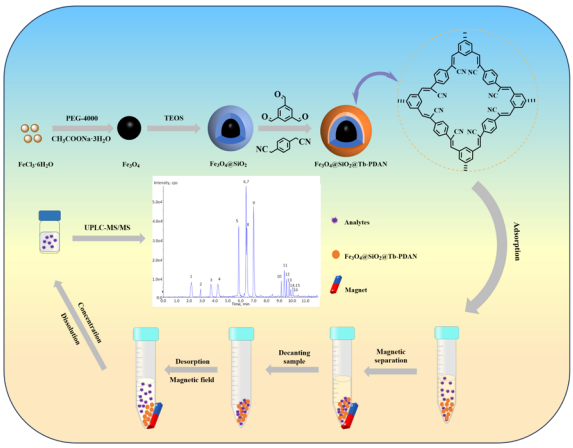

Fig. 1 Scheme illustration for preparation of Fe_3O_4@SiO_2@Tb–PDAN and the MSPE procedure.

3. Results and discussions

3.1. Characterization of the Fe_3O_4@SiO_2@Tb–PDAN

To investigate the microstructure of synthesized materials, the SEM and TEM images of Fe_3O_4 and Fe_3O_4@SiO_2@Tb–PDAN were compared and illustrated in Fig. 2. As shown in Fig. 2a, the structure of Fe_3O_4 showed a smooth and homogeneous surface morphology. However, the SEM image of Fe_3O_4@SiO_2@Tb–PDAN (Fig. 2b) was a relatively rough surface. The same phenomenon could also be observed in TEM images. As depicted in Fig. 2c and d, the Fe_3O_4@SiO_2@Tb–PDAN had a core–shell structure in comparison with Fe_3O_4, which demonstrate the successful formation of Tb–PDAN shell.

The structure of Fe_3O_4@SiO_2@Tb–PDAN could also be confirmed by FT-IR as shown in Fig. 3a. In the spectra, the absorption peaks at 577 and 1105 cm^{-1} were attributed to the vibration of Fe–O–Fe and Si–O–Si, respectively, which are attributed to providing evidence for silica coating of magnetite nanospheres. Otherwise, Fe_3O_4@SiO_2@Tb–PDAN has a strong peak at 1612 cm^{-1} and a weak peak at 2937 cm^{-1}, which can be

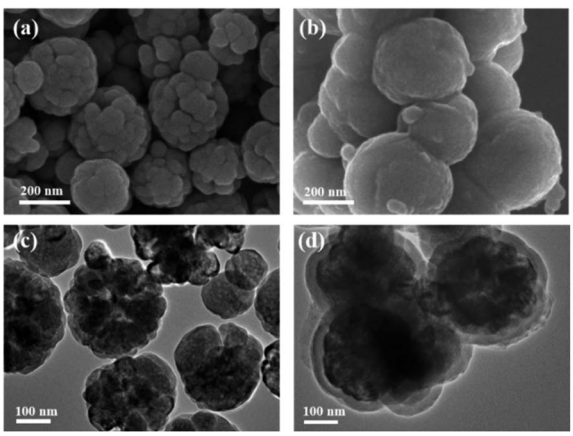

Fig. 2 The SEM image of (a) Fe_3O_4, (b) Fe_3O_4@SiO_2@Tb–PDAN; the TEM image of (c) Fe_3O_4 (d) Fe_3O_4@SiO_2@Tb–PDAN.

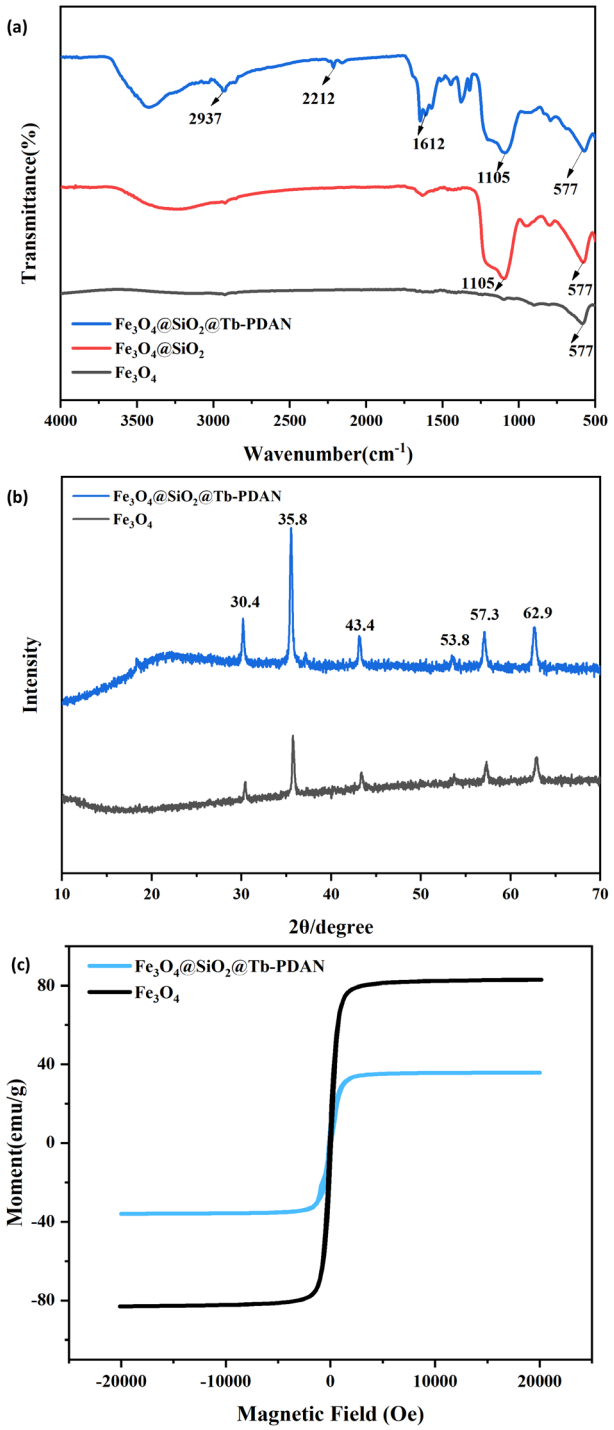

Fig. 3 (a) FT-IR spectra of Fe_3O_4, Fe_3O_4@SiO_2 and Fe_3O_4@SiO_2@Tb–PDAN; (b) XRD patterns of Fe_3O_4 and Fe_3O_4@SiO_2@Tb–PDAN; (c)VSM curves of Fe_3O_4 and Fe_3O_4@SiO_2@Tb–PDAN.

attributed to the stretching vibration of C=C and C=C–H. In addition to this, the characteristic absorption peak of the FT-IR spectrum of Fe_3O_4@SiO_2@Tb–PDAN at 2212 cm^{-1} can be attributed to the –CN. All these results further confirms that Tb–PDAN was successfully coated on the surface of Fe_3O_4@SiO_2.

To ascertain the complexation and crystallization of the polymer matrix, an XRD was used. The results of XRD about the Fe_3O_4 and Fe_3O_4@SiO_2@Tb–PDAN were shown in Fig. 3b. Fe_3O_4@SiO_2@Tb–PDAN presented 6 characteristic peaks with 2θ, consisting of the crystal indexes of (220), (311), (400), (422), (511) and (440) of the Fe_3O_4.[49] The broad peak at 20–30° is probably attributed to π–π interaction between the Tb–PDAN layers of Fe_3O_4@SiO_2@Tb–PDAN.[50] These facts indicated that the Tb–PDAN shell was successfully constructed without destroying the crystalline phase of Fe_3O_4.

The magnetic strength of a magnetic substance is essential to separate it from a liquid medium. Consequently, the magnetic properties of Fe_3O_4 and Fe_3O_4@SiO_2@Tb–PDAN were evaluated. According to Fig. 3c the saturation magnetization of Fe_3O_4@SiO_2@Tb–PDAN was 35.83 emu g^{-1}, which is significantly lower than Fe_3O_4 due to the non-magnetic coating of SiO_2 and Tb–PDAN. However, the saturation magnetization was still sufficient to separate the magnetic nanospheres from the solution.

3.2. Condition of MSPE

3.2.1. Effect of adsorbent dosage. The dosage of adsorbent is a key factor affecting the efficiency of MSPE. The effects of 6, 8, 10, 12 and 14 mg Fe_3O_4@SiO_2@Tb–PDAN on the recoveries of MALs were compared. As indicated in Fig. 4a, when the mass of the adsorbent was increased from 6 mg to 12 mg, the recoveries was improved. Over 12 mg, most of the recoveries remained unchanged. Aimed to ensure sufficient adsorption sites and save material, the optimum absorbent dosage was determined to be 12 mg.

3.2.2. Effect of sample solution pH. MALs are weakly basic compounds, and their glycosidic bonds are easily hydrolyzed under acidic conditions (pH < 4) and cracked central rings under alkaline conditions (pH > 9),[51] which affects the extraction efficiency. By adding an appropriate amount of formic acid or ammonia, the adsorption of MALs was investigated Fe_3O_4@SiO_2@Tb–PDAN at pH 3, 5, 7, 8, 9 and 11, respectively, as shown in Fig. 4b, the recoveries of clindamycin and erythromycin was less than 20.00% at pH = 3. With the increase of pH, the overall recoveries of 16 MALs have increased. And the recoveries were the best when pH = 8, at 62.10–106.65%. When the pH continued to increase to 11, nearly half of the targets had recoveries of less than 50.00%. Therefore, for MSPE, the pH of sample solution was adjusted to 8.

3.2.3. Effect of salt concentration. On the one hand, adding salt will increase the density and viscosity of the solution, which is unfavorable to adsorption. On the other hand, the addition of salt can increase the ionic strength of the sample solution, thus reducing the solubility of the analytes in the sample solution through the salt-out effect, which is conducive to adsorption.[52] To investigate the effect of salt addition on the adsorption and get the best efficiency, different concentrations of NaCl solution (0–20%, w/v) were optimized. As shown in Fig. 4c, as the salt concentration increases, the extraction recoveries for most MALs have no significant changes. This may be due to the hydrophobic nature of the MALs. Therefore, further experiments were performed without NaCl addition.

3.2.4. Effect of extraction time. The interaction time between the adsorbent and analytes was another important

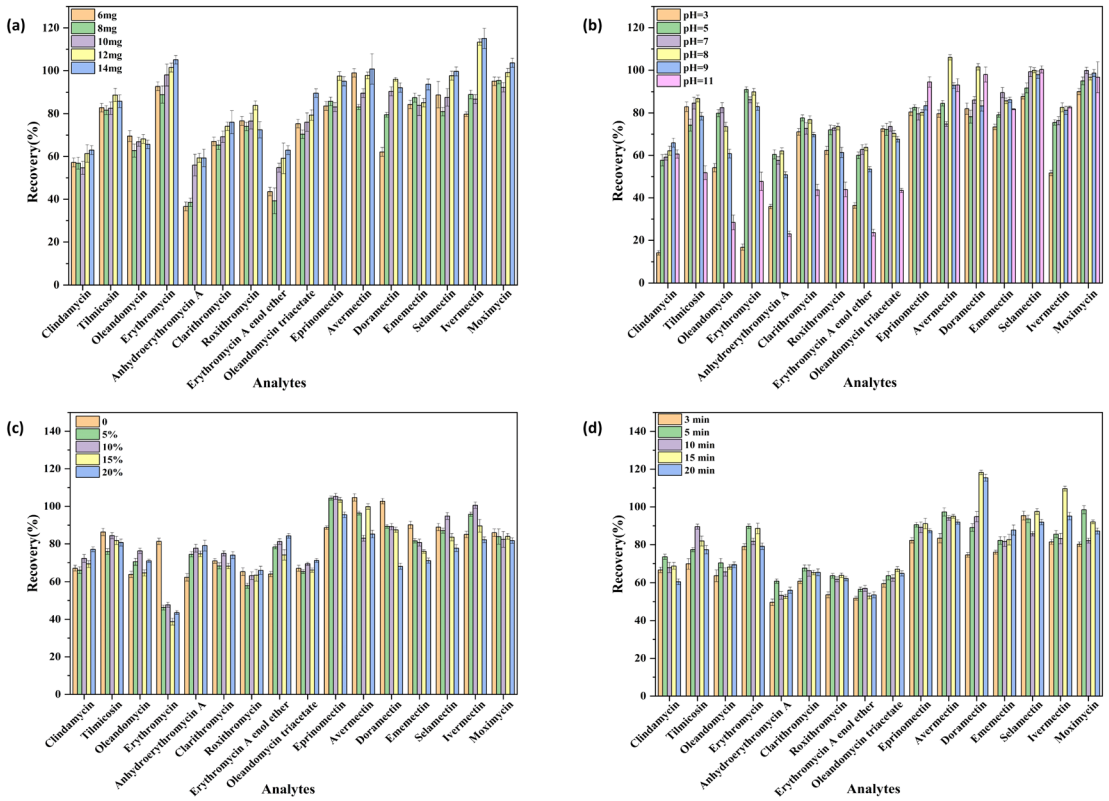

Fig. 4 Effect of (a) adsorbent dosage; (b) sample solution pH; (c) salt concentration; (d) extraction time.

factor affecting extraction efficiency since MSPE is a time-dependent equilibrium process. For the experiment, it was studied for periods ranging from 3 to 20 min. As can be seen from Fig. 4d, the overall recovery was better at an extraction time of 5 min. Further extension of extraction time did not have a significant impact on the improvement of extraction efficiency. Herein, 5 min extraction time was adopted.

3.2.5. Investigation of desorption parameters. The type of eluent plays a significant role in the extraction process. In this study, different types of organic solvents including AC, MA, ACN, and ammoniated ACN were chosen for comparison. Fig. 5a showed that 0.3% ammoniated ACN possessed the best extraction efficiencies toward to the 16 MALs. Therefore, 0.3% ammoniated ACN was used as the eluent. In addition to eluent, elution volume as an important parameter was optimized ranging from 4 to 7 mL. The recoveries increased with the increasing of elution volume from 4 to 7 mL and then basically did not change. The results showed that the recoveries reached the highest when the eluent was 6 mL (Fig. 5b). Therefore, 6 mL of eluent was used in further experiments. Furthermore, the desorption time also affects the extraction efficiencies, which could be examined by the vortex time. The results indicated that 5 min (Fig. 5c) was enough for the MALs desorption. Finally, 5 min vortex time was adopted.

3.2.6. Effect of change in Tb–PDAN concentration on surface of Fe_3O_4@SiO_2. The loading of Tb–PDAN to Fe_3O_4@SiO_2 at different concentrations can provide more insight into the role of the adsorbent in adsorption. In the experiment, the loading of Tb–PDAN at three concentrations on surface of Fe_3O_4@SiO_2 was investigated. As shown in the Table S5,† the adsorption rate (26.73–62.48%) was significantly lower at the low concentration. At the medium concentration, the material exhibited good magnetism, easy separation and recovery. The adsorption rate at this concentration is 71.74–96.10%. At the high concentration, the adsorption rate (70.82–96.32%) did not increase significantly. This may be due to the excessive loading of Tb–PDAN, which reduced the magnetism of the material, making it difficult to recover and resulting in losses. Therefore, loading the medium concentration of Tb–PDAN was chosen for the experiment.

3.3. Adsorption mechanism

The adsorption mechanisms of Fe_3O_4@SiO_2@Tb–PDAN for MALs may be attributed to multiple interactions. On the one hand, Fe_3O_4@SiO_2@Tb–PDAN contains cyano groups and benzene rings. Cyano groups are electron-rich groups and they established conjugation with the benzene rings. This conjugation enhances the electron cloud density, which facilitates the creation of strong intermolecular forces between Fe_3O_4@SiO_2@Tb–PDAN and the MALs, leading to enhanced adsorption. Furthermore, based on the structure of C=O of MALs and the large π-conjugation system of Fe_3O_4@SiO_2@Tb–PDAN, we speculated that π–π interactions played an important role in the adsorption process. Fig.S3† showed that the adsorption performance of Fe_3O_4@SiO_2@Tb–PDAN on MALs was much

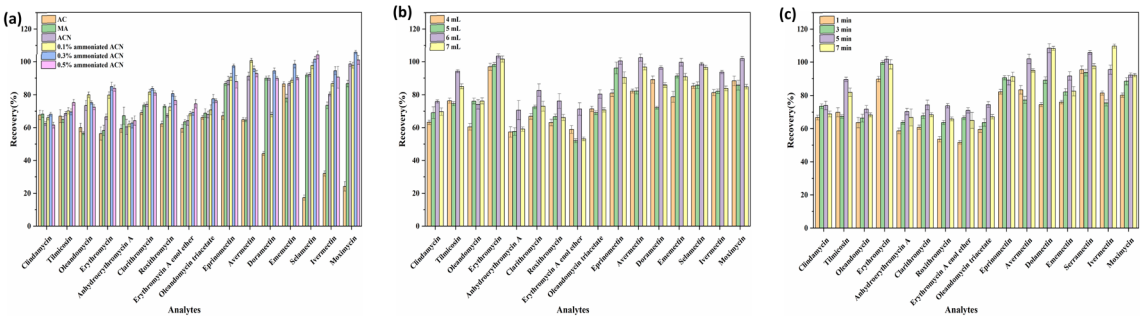

Fig. 5 Effect of (a) type of eluent; (b) elution volume; (c) desorption time.

better than that of Fe_3O_4@SiO_2, which suggested that the addition of Tb–PDAN can significantly enhance the adsorption ability of MALs. In addition, MALs have hydrogen bonding sites (oxygen atoms),[44] Fe_3O_4@SiO_2@Tb–PDAN has cyano groups, suggesting that the hydrogen bonding interaction should be the adsorption mechanism. On the other hand, the structure of Fe_3O_4@SiO_2@Tb–PDAN contains a large proportion of hydrocarbon groups, so it is hydrophobic. According to the principle of "like dissolves like", MALs and Fe_3O_4@SiO_2@Tb–PDAN are more likely to interact in an aqueous environment. To investigate the possible adsorption mechanisms and selectivity of Fe_3O_4@SiO_2@Tb–PDAN for analytes, it was used for MSPE of four types of analytes including MALs, sulfonamides (SAs), β-lactams (β-LAs) and quinolones (QNs). As shown in Table S6,† the Fe_3O_4@SiO_2@Tb–PDAN showed the highest extraction recoveries for MALs (71.54–98.29%) while the lowest recoveries for SAs (0.71–1.49%). The recoveries for β-LAs and QNs were 2.51–5.26% and 27.86–31.23%. From their log K_{ow} values of 1.23–8.43 (MALs), 0.84–1.22 (QNs), 0.59–0.69 (β-LAs) and 0.03–0.07 (SAs), the recoveries increased with the increase of the log K_{ow} values, indicating that hydrophobic interaction may contribute a lot for the good extraction efficiency of Fe_3O_4@SiO_2@Tb–PDAN toward the 16 MALs.[53,54] Hence, it can be deduced the interaction mechanism between MALs and Fe_3O_4@SiO_2@Tb–PDAN was intermolecular forces and hydrophobic interactions.

3.4. Reusability of the adsorbent

To assess the efficiency and stability of the adsorbent, reusability was investigated as an important factor in extraction. Herein, Fe_3O_4@SiO_2@Tb–PDAN that went through the adsorption–desorption process was washed with 0.3% ammoniated ACN. It was then dried under vacuum at 60 °C for 4 h before the next use. Fig. S2† demonstrated that the adsorbent was used three times without a significant decline for the recoveries of MALs, which proved Fe_3O_4@SiO_2@Tb–PDAN is an adsorbent with good reusability.

3.4.1 Matrix effect. Matrix effects were assessed by the ratio of slopes between the matrix-matched calibration curves and the solvent calibration curves. ME < 80.0% indicated matrix inhibition, whereas its >120.0% indicated matrix enhancement effect. When ME was between 80.0% and 120.0%, the matrix effect could be ignored. For water samples, the matrix effects were in the range of 85.9–117.6%. And for honey samples, they were in the range of 80.0–119.7%. Both of samples, the matrix effects were within 80.0–120.0%, as shown in Table S3.† Thus, there was a negligible matrix effect.

3.5. Method validation

The analytical performance of the developed MSPE-LC-MS/MS method was evaluated under the optimal conditions. The linear range was 0.1–200 μg L^{-1} with the correlation coefficient more than 0.999. The limits of detection (LODs) and the limits of quantification (LOQs) were calculated based on a signal/noise ratio (S/N) of 3 and 10, respectively. For water sample, the LODs of 16 MALs were in the range of 0.001–0.012 μg L^{-1} and the LOQs were in the range of 0.002–0.038 μg L^{-1}. For honey sample, the LODs of 16 MALs were in the range of 0.001–0.367 μg kg^{-1} and the LOQs were in the range of 0.003–1.222 μg kg^{-1}. The results of analytical performance for 16 MALs were listed in Table S4.†

The accuracy of the method was evaluated by measuring recoveries different concentrations of target compounds. Precision of the method was expressed by relative standard deviation (RSD). Table 1 showed the recoveries and three spiked concentrations of the 16 MALs in water as well as honey samples. It expressed the recoveries ranged from 71.03–117.2% for water samples with RSD 0.99–9.45%. Recoveries of honey samples were in the range of 70.02–118.91% with RSD 1.72–10.00%. In addition, the adsorption capacity of the Fe_3O_4@SiO_2@Tb–PDAN for MALs was investigated by measuring a set of spiked water samples with different concentration, and the capacity of the adsorbent was 652.21 μg g^{-1}, which displayed good adsorption ability.

3.6. Method application in real samples

20 water samples and 15 honey samples were determined by the method established in this study. In two of the water samples, tilmicosin and roxithromycin were detected. The content of tilmicosin was 23.7 μg L^{-1} and roxithromycin was 0.125 μg L^{-1}. Otherwise, Anhydroerythromycin A was detected in honey samples at 0.48 μg kg^{-1}. Consequently, although MRLs for water and honey are not yet regulated by the various standard-setting organizations, this should be taken into account.

Table 1 The recovery analysis of 16 MALs in real samples ($n = 5$)

	Water sample			Honey sample		
Analytes	Spiked (μg L^{-1})	Recovery (%)	RSD (%)	Spiked (μg kg^{-1})	Recovery (%)	RSD (%)
Clindamycin	0.1	91.54	3.10	20	77.69	9.39
	2	83.41	1.79	100	90.38	4.14
	10	80.04	5.13	500	89.88	4.89
Tilmicosin	0.1	91.32	7.51	20	82.13	9.69
	2	101.01	6.65	100	105.41	8.20
	10	87.94	4.63	500	83.28	10.00
Oleandomycin	0.1	83.10	2.86	20	74.34	9.81
	2	75.35	6.44	100	89.09	8.52
	10	75.59	1.92	500	97.55	3.92
Erythromycin	0.1	100.44	2.33	20	76.02	9.94
	2	107.50	3.28	100	86.79	3.98
	10	107.33	2.73	500	83.07	1.72
Anhydroerythromycin A	0.1	72.74	2.59	20	75.16	6.79
	2	73.01	7.54	100	97.72	6.03
	10	71.03	4.14	500	97.34	3.95
Clarithromycin	0.1	79.40	3.63	20	74.02	5.15
	2	74.30	7.36	100	84.77	4.76
	10	82.84	8.08	500	83.48	8.67
Roxithromycin	0.1	84.18	7.97	20	73.60	9.96
	2	73.52	2.21	100	88.40	8.85
	10	86.73	7.98	500	83.49	8.28
Erythromycin A enol ether	0.1	71.71	8.76	20	72.79	9.49
	2	71.24	7.41	100	88.21	5.06
	10	82.66	6.88	500	97.41	6.33
Oleandomycin triacetate	0.1	81.41	8.99	20	77.10	7.08
	2	92.38	3.94	100	86.66	7.51
	10	74.78	8.07	500	92.43	6.17
Eprinomectin	0.1	86.92	7.02	20	72.28	8.37
	2	82.04	7.13	100	70.02	9.33
	10	74.96	8.96	500	70.78	8.97
Avermectin	0.1	105.36	6.28	20	70.28	6.08
	2	96.31	7.54	100	109.59	9.22
	10	117.20	9.45	500	115.83	9.49
Doramectin	0.1	92.88	2.25	20	117.68	7.74
	2	94.35	1.65	100	118.63	9.36
	10	72.58	7.32	500	117.21	6.26
Ememectin	0.1	75.09	4.15	20	118.91	9.19
	2	80.48	5.87	100	116.12	7.98
	10	98.21	8.73	500	109.98	9.79
Selamectin	0.1	98.24	0.99	20	80.62	9.88
	2	99.65	9.87	100	81.23	9.69
	10	98.33	5.63	500	76.15	9.26
Ivermectin	0.1	96.85	4.13	20	72.16	8.60
	2	93.64	7.55	100	72.19	8.88
	10	111.53	3.25	500	88.29	9.16
Moximycin	0.1	102.03	3.46	20	78.33	9.61
	2	101.10	1.71	100	93.47	3.43
	10	104.27	5.32	500	85.87	5.18

3.7. Comparison with other methods

The performance of the proposed method was compared with other reported methods for the determination of MALs residues in terms of sample pretreatments, analytical method, sample matrix, extraction time, recovery and LODs. The results are presented in Table 2. As can be seen, LC-MS/MS was the most used analytical method for the detection of MALs. The maximum number of MALs detected was 7 in the reported methods and each method focused on the analysis of a single sample types. In comparison, the method in this work was used for the detection of 16 MALs, which was successfully applied to the detection in two types of samples. Besides, the extraction time of the method was faster than that of most reported methods.[15,55,56] Only a method exhibited the same extraction time but slightly lower recoveries.[11] The LODs with the current method were lower and the recoveries was comparatively high. The above comparison showed the proposed new method has

Table 2 Comparison with other methods for the determination of MALs published in the literature

Pretreatment	Analytical method	Sample	Analyte	Extraction time	Recovery (%)	LODs	Ref.
MSPE	LC-MS/MS	Water	4 MALs	5 min	54–117	0.011–0.026 μg L^{-1}	11
DSPE	HPLC-MS/MS	Honey	7 MALs	20 min	88.0–117	0.003–0.017 μg kg^{-1}	15
SPE	LC-MS/MS	Chicken	6 MALs	50 min	82.1–101.4	0.20–0.50 μg kg^{-1}	55
MSPE	HPLC	Water	5 MALs	30 min	92.9–108.7	3.1–44.6 μg kg^{-1}	56
MSPE	LC-MS/MS	Water	16 MALs	5 min	71.03–117.2	0.001–0.012 μg L^{-1}	This work
		Honey			70.02–118.9	0.001–0.367 μg kg^{-1}	

the advantages of easy operation, considerable recoveries and the low LODs for determining MALs in water and honey samples.

4. Conclusions

In this study, a novel magnetic organic polymer Fe_3O_4@SiO_2@Tb–PDAN containing the cyano groups and C=C conjugated structure was successfully prepared, which can be utilized to effectively extract 16 MALs from water and honey samples. The magnetic polymer has advantages such as good magnetism, easy separation and reusability. Using Fe_3O_4@SiO_2@Tb–PDAN as the adsorbent, an MSPE-LC-MS/MS method was developed for the simultaneous and high-throughput analysis of 16 MALs, which exhibited high sensitivity, wide linear range, easy operation and good accuracy. Importantly, this method can provide technical support for the surveillance of MALs in water and food.

Author contributions

Mengnan Liang: conceptualization, formal analysis, methodology, writing – original draft. Na Li: data curation, formal analysis. Hao Zhang: methodology, validation. Ling Ma: conceptualization, supervision, funding acquisition. Ke Wang: conceptualization, funding acquisition, project administration, resources, writing – review & editing. All authors have read and agreed to the published version of the manuscript.

Conflicts of interest

There are no conflicts to declare.

Acknowledgements

This work was supported by the National Natural Science Foundation of China (81903322), S&T Program of Hebei (223777116D).

References

1 G. P. Dinos, *Br. J. Pharmacol.*, 2017, **174**, 2967–2983.
2 N. Farmer, V. Hodgetts-Morton and R. K. Morris, *Eur. J. Obstet. Gynecol. Reprod. Biol.*, 2020, **244**, 163–171.
3 A. G. Myers and R. B. Clark, *Acc. Chem. Res.*, 2021, **54**, 1635–1645.
4 J. Pollock and J. D. Chalmers, *Pulm. Pharmacol. Ther.*, 2021, **71**, 102095.
5 A. Pani, M. Lauriola, A. Romandini and F. Scaglione, *Int. J. Antimicrob. Agents*, 2020, **56**, 106053.
6 M. Kyprianou, K. Dakou, A. Aktar, H. Aouina, N. Behbehani, K. Dheda, G. Juvelekian, A. Khattab, B. Mahboub, G. Nyale, S. Oraby, A. Sayiner, A. Shibl, M. A. T. El Deen, S. Unal, A. B. S. Zubairi, R. Davidson and E. J. Giamarellos-Bourboulis, *Int. J. Antimicrob. Agents*, 2023, **62**, 106942.
7 G. El-Saber Batiha, A. Alqahtani, O. B. Ilesanmi, A. A. Saati, A. El-Mleeh, H. F. Hetta and A. Magdy Beshbishy, *Pharmaceuticals*, 2020, **13**, 196–232.
8 G. E. Agga, H. O. Galloway, K. Appala, F. Mahmoudi, J. Kasumba, J. H. Loughrin and E. Conte, *Prev. Vet. Med.*, 2023, **215**, 105930.
9 M. Zieliński, J. Park, B. Sleno and A. M. Berghuis, *Nat. Commun.*, 2021, **12**, 1732.
10 A. Diana, M. Santinello, M. Penasa, F. Scali, E. Magni, G. L. Alborali, L. Bertocchi and M. De Marchi, *Prev. Vet. Med.*, 2020, **181**, 105032.
11 R. A. Perez, B. Albero, M. Ferriz and J. L. Tadeo, *J. Pharm. Biomed. Anal.*, 2017, **146**, 79–85.
12 J. Li, W. Li, K. Liu, Y. Guo, C. Ding, J. Han and P. Li, *J. Hazard. Mater.*, 2022, **439**, 129628.
13 I. Senta, S. Terzić and M. Ahel, *Chromatographia*, 2008, **68**, 747–758.
14 M. L. Gomez-Perez, P. Plaza-Bolanos, R. Romero-Gonzalez, J. L. Martinez-Vidal and A. Garrido-Frenich, *J. Chromatogr. A*, 2012, **1248**, 130–138.
15 S. Ji, T. Li, W. Yang, C. Shu, D. Li, Y. Wang and L. Ding, *Microchim. Acta*, 2018, **185**, 203–211.
16 R. Cañadas, R. M. Garcinuño Martínez, G. Paniagua González and P. Fernández Hernando, *Polymer*, 2022, **249**, 124843.
17 Q. Wu, M. A. B. Shabbir, D. Peng, Z. Yuan and Y. Wang, *Food Chem.*, 2021, **363**, 130074.
18 M. Hu, Y. Ben, M. H. Wong and C. Zheng, *J. Agric. Food Chem.*, 2021, **69**, 1656–1666.
19 Y. Tao, G. Yu, D. Chen, Y. Pan, Z. Liu, H. Wei, D. Peng, L. Huang, Y. Wang and Z. Yuan, *J. Chromatogr. B: Anal. Technol. Biomed. Life Sci.*, 2012, **897**, 64–71.
20 A. Moga, M. Vergara-Barberan, M. J. Lerma-Garcia, E. J. Carrasco-Correa, J. M. Herrero-Martinez and E. F. Simo-Alfonso, *Compr. Rev. Food Sci. Food Saf.*, 2021, **20**, 1681–1716.

21 J. D. Smilack, W. R. Wilson and F. R. Cockerill, *Mayo Clin. Proc.*, 1991, **66**, 1270–1280.
22 Z. Yan, X. Huang, Y. Xie, M. Song, K. Zhu and S. Ding, *Sci. Total Environ.*, 2019, **649**, 1414–1421.
23 K. Ikuta, S. Nakagawa, C. Yamawaki, K. Itohara, D. Hira, S. Imai, A. Yonezawa, T. Nakagawa, M. Sakuragi, N. Sato, E. Uchino, M. Yanagita and T. Terada, *BMC Nephrol.*, 2022, **23**, 383–391.
24 Y. Zhou, T. Zhou, H. Jin, T. Jing, B. Song, Y. Zhou, S. Mei and Y. I. Lee, *Talanta*, 2015, **137**, 1–10.
25 A. S. Lorenzetti, A. G. Lista and C. E. Domini, *LWT*, 2019, **113**, 108334.
26 X. Li, K. Wen, Y. Chen, X. Wu, X. Pei, Q. Wang, A. Liu and J. Shen, *Food Anal. Methods*, 2015, **8**, 2368–2375.
27 M. Ali, S. T. H. Sherazi and S. A. Mahesar, *Arab. J. Chem.*, 2014, **7**, 1104–1109.
28 I. Varenina, N. Bilandžić, Đ. B. Luburić, B. S. Kolanović, I. Varga, M. Sedak and M. Đokić, *Food Control*, 2023, **148**, 109676.
29 S. Ghareghani, S. Goudarzi, M. Amirahmadi, S. Kheirandish, H. Ghafari, B. Daraei and M. Ghazi-Khansari, *Int. Dairy J.*, 2023, **137**, 105506.
30 S. N. Thomas, D. French, P. J. Jannetto, B. A. Rappold and W. A. Clarke, *Nat. Rev. Methods Primers*, 2022, **2**, 96.
31 R. P. Lopes, D. V. Augusti, A. G. M. Oliveira, F. A. S. Oliveira, E. A. Vargas and R. Augusti, *Food Addit. Contam.: Part A*, 2011, **28**, 1667–1676.
32 K.-Y. Chen, T. C. Yang and S. Y. Chang, *J. Am. Soc. Mass Spectrom.*, 2012, **23**, 1157–1160.
33 S. Liu, J. Zong, Z. Wei, H. Zhang, L. Bai, H. Liu and H. Yan, *J. Appl. Polym. Sci.*, 2016, **133**, 43943.
34 N. Razavi and A. Sarafraz Yazdi, *J. Sep. Sci.*, 2017, **40**, 1739–1746.
35 Z. Liu, H. Zhao, J. Wang, Z. Wang, S. Di, H. Xu, Q. Wang, X. Wang, X. Wang and P. Qi, *Food Chem.*, 2023, **400**, 134036.
36 H.-L. Jiang, N. Li, L. Cui, X. Wang and R.-S. Zhao, *TrAC, Trends Anal. Chem.*, 2019, **120**, 115632.
37 M. Mu, S. Zhu, Y. Gao, N. Zhang, Y. Wang and M. Lu, *Talanta*, 2023, **260**, 124540.
38 Y. Li, Z. Yan, J. Fan, X. Yao and Y. Cai, *Talanta*, 2023, **265**, 124916.
39 Y. Wu, J. Xiong, S. Wei, L. Tian, X. Shen and C. Huang, *J. Chromatogr. A*, 2024, **1714**, 464550.
40 S. Jiang, Z. Li, X. Yang, M. Li, C. Wang, Z. Wang and Q. Wu, *Food Chem.*, 2023, **404**, 134652.
41 Y. Yang, Z. Shi, X. Wang, B. Bai, S. Qin, J. Li, X. Jing, Y. Tian and G. Fang, *Food Chem.*, 2022, **395**, 133532.
42 H. Wang, X. Zhao, J. Xu, Y. Shang, H. Wang, P. Wang, X. He and J. Tan, *J. Chromatogr. A*, 2021, **1651**, 462286.
43 J. Yu, B. Wang, J. Cai, Q. Yan, S. Wang, G. Zhao, J. Zhao, L. Pan and S. Liu, *RSC Adv.*, 2020, **10**, 28437–28446.
44 M. Li, W. Liu, X. Meng, S. Li, Q. Wang, Y. Guo, Y. Wu, L. Hao, X. Yang, Z. Wang, C. Wang and Q. Wu, *Food Chem.*, 2022, **395**, 133596.
45 X.-Q. He, Y.-Y. Cui and C.-X. Yang, *Talanta*, 2021, **224**, 121876.
46 Y. Zhao, R. Wu, H. Yu, J. Li, L. Liu, S. Wang, X. Chen and T. W. D. Chan, *J. Chromatogr. A*, 2020, **1610**, 460543.
47 L. Zhou, S. Pan, X. Chen, Y. Zhao, B. Zou and M. Jin, *Chem. Eng. J.*, 2014, **257**, 10–19.
48 R. Chen, J. L. Shi, Y. Ma, G. Lin, X. Lang and C. Wang, *Angew. Chem., Int. Ed. Engl.*, 2019, **58**, 6430–6434.
49 N. Y. Elamin, A. Modwi, W. Abd El-Fattah and A. Rajeh, *Opt. Mater.*, 2023, **135**, 113323.
50 Z. Hong, Y. Dong, R. Wang, Y. Chen and G. Wang, *J. Chromatogr. A*, 2022, **1678**, 463357.
51 J. Du, X. Li, L. Tian, J. Li, C. Wang, D. Ye, L. Zhao, S. Liu, J. Xu and X. Xia, *Food Chem.*, 2021, **365**, 130502.
52 Y. Guo, J. Wang, L. Hao, Q. Wu, C. Wang and Z. Wang, *J. Chromatogr. A*, 2021, **1649**, 462238.
53 S. Li, W. Liu, Q. Wang, M. Xu, Y. An, L. Hao, C. Wang, Q. Wu and Z. Wang, *Food Chem.*, 2022, **382**, 132362.
54 A. O. Melekhin, V. V. Tolmacheva, N. O. Goncharov, V. V. Apyari, S. G. Dmitrienko, E. G. Shubina and A. I. Grudev, *Food Chem.*, 2022, **387**, 132866.
55 C. Lan, D. Yin, Z. Yang, W. Zhao, Y. Chen, W. Zhang and S. Zhang, *J. Anal. Methods Chem.*, 2019, **2019**, 1–13.
56 Y. Liu, H. Zhang, D. Xie, H. Lai, Q. Qiu and X. Ma, *J. Environ. Chem. Eng.*, 2022, **10**, 108094.